The 12th Laser Display and Lighting Conference (LDC2023,) Yokohama, Japan, April 18–21, 2023.

High-Frequency Homogenization of Laser Illumination Through Stationary 0.22 N.A. Multimode Optical Fiber

Fergal Shevlin
DYOPTYKA, 7 Westland Court, South Cumberland St., Dublin 2, Ireland.
Phone: +353-85-1423747; Email: fshevlin@dyoptyka.com

Abstract: *Our phase-randomizing deformable mirror technology is shown to be effective for homogenization of illumination intensity, and for minimization of speckle, within a camera exposure period of only* 20 µs *when used with 0.22 N.A. multimode optical fiber.*

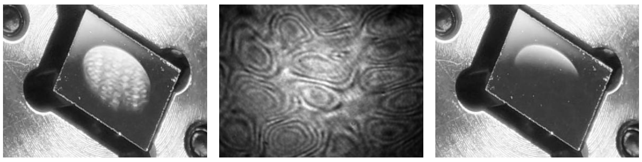

Fig. 1: [Left] Deformable mirror active. Randomly-distributed surface deformations are excited at frequencies up to 1.5 MHz in a 3 mm×4.5 mm elliptical region. Reflectance $\geq$ 95% and damage threshold >1 W mm^{-2} for wavelength-appropriate mirror coatings. [Center] Microscope interferometer image showing fringes resulting from actual mirror deformations. [Right] Mirror surface near planar when inactive.

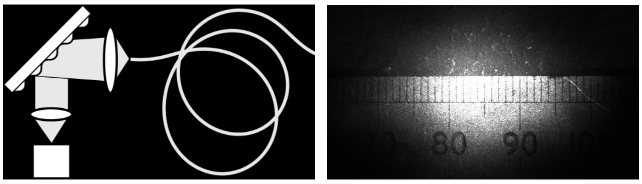

Fig. 2: [Left] Typical deformable mirror optical system for fiber coupling. Light from a laser source is directed into a small area, for example ⌀500 µm, from where it is reflected and focused into a smaller area with a larger angle or vice-versa, in accordance with the optical invariant. [Right] Light is not scattered outside an angular extent proportional to mirror surface deformation amplitude.

1 Introduction

Our company's phase-randomizing deformable mirror technology (see figure 1) is used to reduce speckle and other unwanted interference effects in many applications [1]. Its characteristics make it particularly suitable for optically efficient fiber-coupling, see figure 2. We have already demonstrated its performance with large N.A. multimode fiber, see figure 3 and [2]. Speckle reduction is achieved through spatio-temporal averaging of light that has propagated through different guided modes in the optical fiber. Since the number of modes is proportional to (N.A.)^2 and ⌀^{2}, the question arises whether good performance can be achieved with smaller N.A. fiber. Herein we demonstrate that it is; using 0.22 N.A. multimode fiber

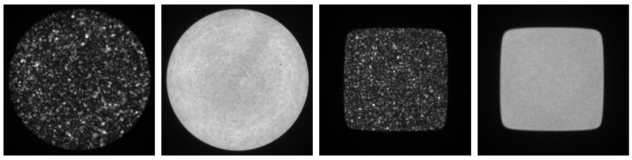

Fig. 3: Exit faces of 0.39 N.A. multimode fiber with deformable mirror inactive and active. [Left pair] Circular core ⌀200 µm. Speckle contrast ratio $C_S = 58.9\%$ and 5.3% respectively. [Right pair] Square core □150 µm. $C_S = 47.5\%$ and 3.6% respectively.

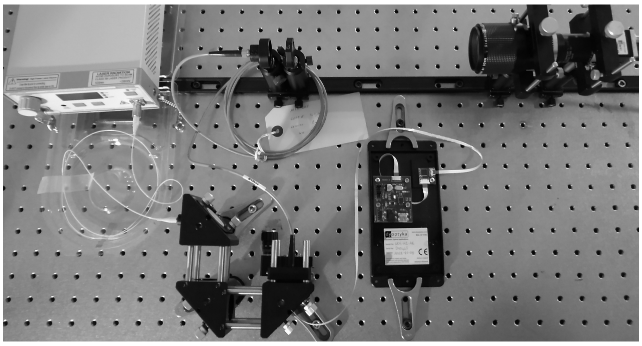

Fig. 4: Emission from Thorlabs S4FC λ=520 nm laser source is coupled into CFS2-532-FC single mode fiber with an f=1.97 mm collimator for an approx. ⌀500 µm beam. Two steering mirrors align beam onto deformable mirror operating with approx. $\pm 1^\circ$ randomized divergence. An F230SMA-A f=4.34 mm collimation package is positioned approx. 10 mm from mirror for approx. $1/2\times$ size and $2\times$ angular magnification into entrance face of 0.22 N.A. multimode optical fiber of length 2 m, coiled and stationary. An F220SMA-A collimation package at the exit face of the fiber directs light through a focusing lens and an f=55 mm imaging lens into a Basler Ace camera for approx. $16\times$ magnification onto the 1920×1080 pixel sensor.

with cores ⌀550 µm, ⌀200 µm, ⌀105 µm, and ⌀50 µm.

2 Apparatus

Some details are provided in figure 4. The sensor exposure period was 20 µs for all image acquisitions which in principle could support a frame rate of 50 kHz. The bending radii of the fiber coils were not all the same.

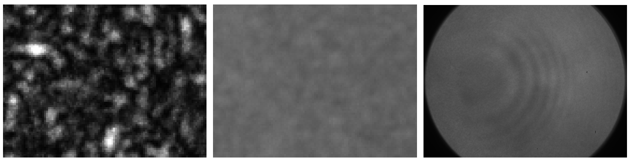

Fig. 5: Regions of exit face of $\varnothing 550\,\mu\mathrm{m}$, 0.22 N.A. multimode fiber. [Left] Deformable mirror inactive, $C_S = 77\%$. [Center] Deformable mirror active, $C_S = 5.2\%$. [Right] Larger region, average of nine images acquired with deformable mirror active, $C_S = 3.6\%$.

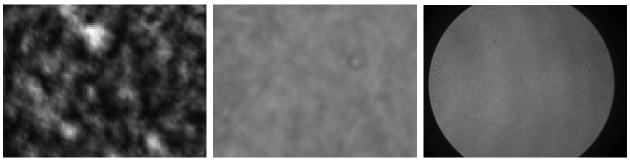

Fig. 6: Regions of exit face of $\varnothing 200\,\mu\mathrm{m}$, 0.22 N.A. multimode fiber. [Left] Deformable mirror inactive, $C_S = 63\%$. [Center] Deformable mirror active, $C_S = 5.5\%$. [Right] Larger region, average of nine images acquired with deformable mirror active, $C_S = 3.8\%$.

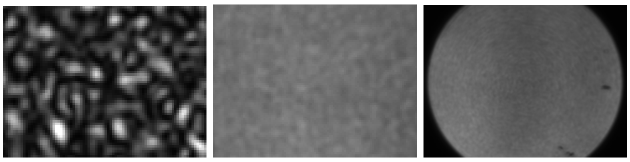

Fig. 7: Regions of exit face of $\varnothing 105\,\mu\mathrm{m}$, 0.22 N.A. multimode fiber. [Left] Deformable mirror inactive, $C_S = 74\%$. [Center] Deformable mirror active, $C_S = 7.1\%$. [Right] Larger region, average of nine images acquired with deformable mirror active, $C_S = 6.9\%$.

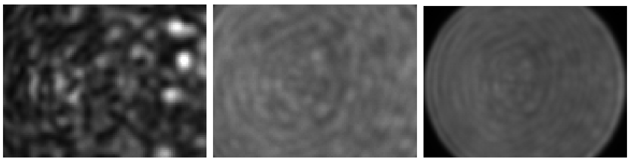

Fig. 8: Regions of exit face of $\varnothing 50\,\mu\mathrm{m}$, 0.22 N.A. multimode fiber. [Left] Deformable mirror inactive, $C_S = 59\%$. [Center] Deformable mirror active, $C_S = 9.7\%$. [Right] Larger region, average of nine images acquired with deformable mirror active, $C_S = 7.8\%$.

This could explain some of the differences in speckle contrast and grain size with deformable mirror inactive, see Figures 5, 6, 7, and 8 [Left].

3 Homogeneity

Figures 5, 6, and 7 [Right] show “Newton’s rings” from the imaging optical system. Figure 8 [Center, Right] shows another kind of irregularity. Hence we felt it inappropriate to quantify uniformity of illumination across the exit faces.

To quantify speckle contrast ratio, we selected 109×82 pixel regions that we judged subjectively to have reasonable uniformity. As can be seen in the imagery, contrast is reduced significantly through the action of the deformable mirror. Smaller cores have higher contrast. However it is noteworthy that the $\varnothing 200\,\mu\mathrm{m}$ fiber faces shown in Figures 3 and 6 have similar contrast ratios despite their different N.A.

To determine whether the sensor’s minimum exposure period of $20\,\mu\mathrm{s}$ was appropriate for the 1.5 MHz deformable mirror frequency, multiple images were averaged and their contrast ratios calculated. The contrast ratios did decrease slightly which implies that better performance could be achieved with longer exposures.

4 Optical Efficiency

With deformable mirror active, the coupling optical system focuses an approx. $\varnothing 350\,\mu\mathrm{m}$ spot at the position of the fiber entrance face. A Thorlabs S142C integrating sphere power meter was used to measure power at the focused spot position and at the exit faces of the different core diameter fibers. For the $\varnothing 550\,\mu\mathrm{m}$ fiber, the power difference was consistent with losses only from the uncoated entrance and exit faces. For the smaller core fibers, the power differences were much greater; consistent with their entrance faces being overfilled by the spot. Such loss should be minimized when the coupling optical system is optimized to underfill the entrance face.

5 Temporal Stability

Although position and size of the focused spot are stable, its intensity profile changes at high frequency. This results in significant variation of transmission efficiency between short exposure periods when the fiber face is overfilled. We used a Thorlabs PDA100A-EC high frequency photodetector at the $\varnothing 550\,\mu\mathrm{m}$ fiber exit face to confirm minimal variation when underfilled.

6 Conclusions

Excellent speckle reduction has been achieved with 0.22 N.A. multimode fiber of various core diameters. Further work will include optimization of coupling for improved transmission efficiency and temporal stability with smaller cores; and an investigation into the influence of fiber length.

[1] Shevlin, F., “Phase randomization for spatio-temporal averaging of unwanted interference effects arising from coherence,” *Applied Optics* **57**(22), E6–E10 (2018).

[2] Shevlin, F., “High-frequency homogenization of laser illumination through stationary multimode optical fiber,” in [*The 11th Laser Display and Lighting Conference (LDC 2022)*], The Japan Society of Applied Physics, Yokohama, Japan (April 2022).

[3] Goodman, J., [*Speckle phenomena in optics*], SPIE, second ed. (2020).